TVTδ Concept for Long-Span Glass–Steel Footbridges

Maurizio Froli[1]; Francesco Laccone[2]; and Agnese Natali[3]

Abstract: Transparency and structural lightness are inspiring ideas in the design of footbridges. Glass is the most performing transparent material to be used for structural purposes because of its high compressive strength, chemical stability, and absence of fatigue and viscosity phenomena at room temperature. However, its fragility constitutes a challenging limit in structural applications. This research provides and discusses a specific concept named TVTδ (Travi Vitree Tensegrity) for lightweight long-span beam-like footbridges made of structural glass. Hence, two design approaches of fail-safe design (FSD) and damage avoidance design (DAD) are applied to guarantee adequate safety levels and postcracking serviceability, respectively, with low damages on the main components. FSD provides the adoption of structural collaboration between glass and steel. Following DAD, glass is segmented into triangular panels, and reciprocal diffuse prestress is performed by steel tendons. This strategy assures low rehabilitation costs because only collapsed elements should be replaced once failed. At ultimate limit state (ULS), the TVTδ footbridge attains a global ductile behavior in which the yielding of steel tendons occurs before any fragile failure. Such result is achieved through a hierarchic calibration of the chain of failures. In glass panels, which are mostly precompressed, the buckling failure, representing the main risk, is delayed by the mutual stabilization of the panels' compressed edges with steel clamping. However, because an accidental event may cause a localized or diffuse brittle failure of glass components, the system is designed to maintain a residual load bearing capacity in this scenario. At the serviceability limit state (SLS), the TVTδ footbridge is highly stiffened by the presence of glass panes, partially encased in metallic frames. Crack initiation is delayed by precompression. **DOI: 10.1061/(ASCE)BE.1943-5592.0001514.**

Author keywords: Structural glass; Fail safe design; Damage avoidance design; Buckling; Post-tensioning.

Introduction

In Search of Transparent Crossing

The contemporary architectural trend to dematerialize structures has brought about structural glass as one of the most interesting transparent materials of recent decades. This is mainly due to its unique characteristic transparency, which mitigates the optical impact of accretions in environmental and cultural heritage sites or confers an iconic character to a building component creating a landmark. Its sense of evanescence in some cases is used to produce vertigo experiences, such as in spectacular transparent walk paths where people can float in the air. This tendency is demonstrated by recent constructions, i.e., the Zhangjiajie Glass Bridge (Dotan 2016), a 385-m glass-bottomed suspended bridge on the namesake Zhangjiajie Grand Canyon in China.

Despite its brittle mechanical behavior, nowadays, glass is the best performing structural material when transparency and durability are requested. It possesses high compressive strength, chemical stability, and absence of viscosity at room temperature. However, these properties are not sufficient to achieve suitable safety levels because surface flaws that are caused by production can propagate if submitted to tensile stress, either instantaneously, if the stress at the tip of one crack exceeds the critical value of fracture toughness, or belatedly, if one subcritical crack grows under sustained load due to so-called static fatigue (Haldimann et al. 2008).

Safety criteria based on stress limitations are not sufficiently descriptive of the postcritical status and cannot guarantee section or element resistance. So, instead of minimizing the probability of failure at a local level, a recommended approach is to minimize the consequences of failure (Bos 2009; Feldmann et al. 2014). Only a smart conceptual design based on robustness, redundancy, and hierarchy, so-called fail-safe design (FSD) criteria, can guarantee enough residual structural capacity in the event of cracking.

This design approach is performance-based. Consequently, the achievable safety level should be raised in challenging applications. Pedestrian glass bridges are excellent examples in which aesthetic and functional outcomes, not least the desire of evanescent walk paths, must be combined with severe safety issues. Few albeit significative glass bridges have to date been investigated or realized. In general terms, it is possible to identify two main categories: massive and lightweight glass bridges.

Massive glass bridges are inspired by classic masonry constructions made of compression-only resisting materials. The idea that glass, which is highly compression resistant, can replace the bricks and the epoxy resin can replace the mortar joints is at the base of the research of Royer-Carfagni and Silvestri (2007), which led to the design of a 50-m footbridge in Venice. Such glass-masonry material in the form of plied glass tiles (laminated or not) was tested experimentally under uniaxial compression, showing noticeable compressive strength (about 90 MPa). Moreover, the lateral stresses of the resins provided the necessary ductility to the specimen assembly, affirming the feasibility of compressed-only footbridges of short and medium spans entirely made of glass.

[1]Professor, Dept. of Energy, Systems, Territory, and Construction Engineering, Univ. of Pisa, 56122 Pisa, Italy.

[2]Research Fellow, Institute of Information Science and Technologies "A. Faedo," National Research Council of Italy, via Giuseppe Moruzzi 1, Pisa 56124, Italy; Dept. of Energy, Systems, Territory, and Construction Engineering, Univ. of Pisa, 56122 Pisa, Italy (corresponding author). ORCID: https://orcid.org/0000-0002-3787-7215. Email: francesco.laccone@isti.cnr.it; francesco.laccone@destec.unipi.it

[3]Ph.D. Student, Dept. of Civil and Industrial Engineering, Univ. of Pisa, 56122 Pisa, Italy.

Note. This manuscript was submitted on December 7, 2018; approved on August 18, 2019; published online on October 25, 2019. Discussion period open until March 25, 2020; separate discussions must be submitted for individual papers. This paper is part of the ***Journal of Bridge Engineering***, © ASCE, ISSN 1084-0702.

If float glass represents the majority of the market, novel structural components made of cast glass are emerging. Hence, molten glass is casted into a mold where it solidifies. Cast glass structures can be realized by gluing cast bricks mutually (such as in the Crystal Houses façade, Oikonomopoulou et al. 2018) or by assembly dry-stacked interlocking cast blocks with thin films of transparent materials. An experimental 14-m-span glass-masonry arch footbridge, whose dry glass-interlayer structural concept was validated on a scale model test by Aurik et al. (2018), is planned to be constructed at the TU Delft Campus.

Lightweight glass bridges are optimized structures from the material usage point of view. A first concept based on the use of laminated glass (LG) panels inspired a pioneering exemplar of transparent footbridge, located in Rotterdam, Netherlands, and designed in 1994 by Nijsse (2003). This footbridge that allows an office to link to another building has a span of approximately 3.50 m and is made of two main parts. The *structural* part is a load bearing layered package of two layers of 15-mm annealed glass, glued onto parabolic glass beams, which are composed by three layers of 10-mm annealed glass. This lower ribbed plate also constitutes the walk path. The *raincoat* part completes the box section of the footbridge and protects users from weather phenomena. Steel connections fix glass walls and roof.

This structure was a source of inspiration for the design of many footbridges that came after, and the statics of the glass stiffened plate and its safety concept are still in use. For increased spans, a U-section can be adopted, i.e., Wittenberg and Krynski (2010). This contribution reports on the design and construction of a pedestrian glass bridge spanning 9.0 m in a hotel lobby. Transversal beams, installed by through-hole connections onto continuous LG balustrades, support the floor plate.

In these types of footbridges, the failure modality of LG avoids sudden collapses but does not allow the structure to undergo large deformations or to manifest visible warning signs. This mechanical behavior is indeed defined as pseudoductile. Moreover, bolted connections are weak points because peak stress, which glass is not able to redistribute plastically, may occur. Especially if the span increases, a fully transparent glass bridge becomes practically not feasible and characterized by a scarce safety level. As in reinforced concrete structures, a new idea for reinforcing glass appeared (Martens et al. 2015a, b; Louter et al. 2012). The aim was to bridge the cracks of glass and to confer the necessary ductile behavior to the glass element. Based on this concept, a special bridge was designed and tested in 2003 by Veer et al. (2003). The 8-m-span U-section glass structure, which is reinforced by two stainless steel profiles located at the section corners, would have served as an aquarium. The webs and the lower plate were realized by adhesively bonding glass segments.

Feng et al. (2015) introduced a concept named glass cable truss for web trusses to be used in pedestrian bridges, supporting a transparent walkway. In such assembly, the cross cables in usual cable trusses are replaced by LG panels, thus bending moment is transferred by upper and lower pre-tensioned cables, while the shear force is transferred by the LG web plates. In this concept, cables are independently prestressed and there is no interaction with glass, which is successively assembled.

Other materials can be also used in collaboration with glass. Vallee et al. (2016), for example, proposed a segmented glass-timber composite pedestrian bridge of 10 m span. The overall design is derived from a Vierendeel beam, in which web profiles are substituted by segmented LG panels. The latter are adhesively bonded on the timber rectangular profiles.

In a hybrid component, the reinforcement, or more generally the added ductile material, can otherwise play a more active role if it has the ability to transfer the prestress loading to glass. Thus, a beneficial compressive eigenstress that delays crack initiation can be superimposed to glass stress state (Bos et al. 2004; Cupać et al. 2017). This expedient was applied by researchers from the Technische Universität Dresden (Engelmann and Weller 2016) in the development of the Spannglass concept for beams and footbridges. Hence, two rectangular LG webs made of 12-mm tempered glass with polyvinyl butyral (PVB) interlayer are assembled in parallel; their extremities are glued on steel connectors creating a partial box section. Both bearing capacity and postbreakage behavior are enhanced by a post-tensioned 24-mm spiral cable with polygonal path.

Background and Objectives of the Present Research

The present research proposes a novel concept for a lightweight beam-like footbridge for medium spans (Fig. 1). Originating from

Fig. 1. Overall render view of a 30-m span TVTδ footbridge.

J. Bridge Eng., 2020, 25(1): 04019117

an unconventional interpretation of the FSD principles, the TVTδ technique is indeed the latest evolutionary step of the Travi Vitree Tensegrity (TVT) system, invented and patented by the first author for the University of Pisa. Full-scale TVT beam prototypes (up to 12 m) were analyzed and tested up to failure, and subjected to static, quasi-static, and dynamic loadings. The main technical and experimental outcomes are briefly recalled in the following.

The TVTδ footbridge is a hybrid, segmented, post-tensioned, buckling-restrained glass-steel structure, with a closed V section. Its mechanical behavior, based on FSD and damage avoidance design (DAD), leads to a ductile ultimate limit state (ULS) failure, obtained by yielding of the lower cables. Segmentation of glass does not allow propagation of damage, and only limited parts of the assembly must be replaced if failed. The overall bearing capacity is designed to preserve also the robustness and redundancy.

The serviceability limit state (SLS) is governed by glass decompression, namely where compressive stresses induced by post-tensioning are not exceeded by tensile stresses caused by external loading. Thus, until the SLS, theoretically no tensile stresses may open the flaws since the panels are still embedded within their casing. And, even after such limit, the glass-to-metal contact being a compression-only restraint, glass can detach from the casing, avoiding relevant tensile stresses.

In the following, a 30-m TVTδ footbridge design case is described. In order to state its feasibility, mechanical performances are evaluated through finite-element (FE) numerical models, calibrated on the experimental data sets of previous TVT prototypes. The present TVTδ concept is rooted in a more general framework of reinforced and post-tensioned glass structures (Froli and Laccone 2018a), which applies also to shells or single-layered structures with high geometric complexity (Froli and Laccone 2018b; Laccone 2019).

TVTδ Structural Concept and Evolution

Original Idea and Qualitative Mechanical Behavior of TVT Beams

To realize a high-performing structural system made of glass, tensile stresses should be absent or negligible, connections should be free from holes or indented edges, and glass should be prevalently submitted to compressive stresses. Surprisingly, these fundamental prerequisites can be satisfied by abandoning the concept of glass structural continuity, which is usually pursued in common splice-laminated glass beams, and adopting the opposite concept of glass partition or segmentation. Inspired by the crack patterns in the webs of a collapsed glass beams, the TVT introduces segmentation of glass as a modular Warren-like partition of the web. Thus, in this segmented setup, crack propagation is prevented.

TVTs are dual-layered structures in which individually laminated triangular glass panels with rounded vertices are inserted free from bolts and bondings into concentric shoe-shaped slots that are cut into the steel nodes. Only contact pressures can be transmitted at the interface between the two materials. A soft material is interposed to avoid localized contact stress peaks. The tensile integrity of the whole assembly is obtained just by means of mutual prestress, exerted during the assembly phase by post-tensioning a net of diagonal and longitudinal unbonded steel cables or bars, which are anchored at the steel nodes (Fig. 2). Hence the acronym TVT (Travi Vitree Tensegrity).

Three main common phases can be distinguished in the mechanical behavior of a TVT. Prestress (Phase 0) confers the glass-steel interface an apparent tensile strength able to balance

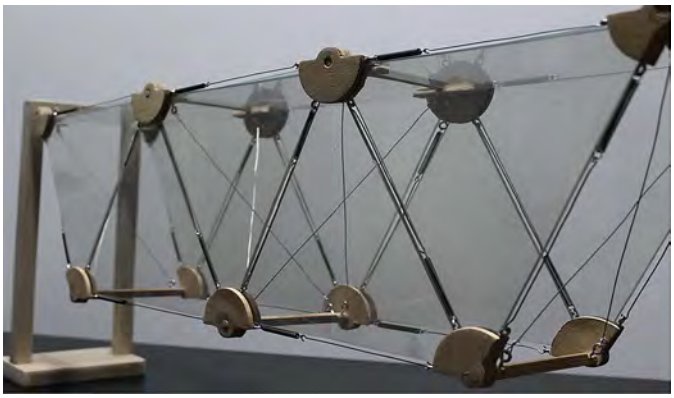

Fig. 2. Original physical scale mock-up of a TVT beam. (Image by Maurizio Froli.)

tensile stresses at the lower side of the beam due to bending as long as the decompression boundary at SLS is reached. From this point forward (Phase 1), the interfaces can detach, and no tension can be further transmitted to glass. If the panels are initially subjected to an isotropic compressive stress, new load paths develop within the panels while live loads increase. Compression spreads around the compressed diagonals, higher nodes and upper flange; and only accompanying negligible tensile stresses due to second-order effects appear. Thus, glass is theoretically preserved from any cracking because tensile bending stresses at the bottom side are entirely sustained by the steel tendons, and tensile shear stresses by diagonal cables (or bars), like in a reticulated Warren lattice.

At ULS (Phase 2), the failure of the structure is identified by the yielding of the lower steel tendons. On the other hand, either the glass brittle failure or buckling of the compressed parts is delayed. Paradoxically, the global failure of a glass structure is brought in the ductile domain and satisfies the FSD principle of hierarchy. This is one of the most innovative features of the TVT system because, unlike other reinforced and post-tensioned glass concepts, the ductile behavior develops before the collapse of glass.

The FSD requirement of redundancy applies in the TVT system at a multiscale level. At the material level, glass sheets are submitted to tempering treatments to provide the outer glass surfaces a beneficial additional compressive eigenstress with the aim of further increasing the superficial tensile strength. At the local level, each panel is composed by two LG sheets, so if the one accidentally fails, the other can bear the load. At the global level, the web of the beam is composed of two in-parallel assembled LG packages. Similarly, if one of the web panels completely collapses, the other provides an alternative load path for carrying loads, with albeit reduced safety reserves. Most importantly, the repair works can be easily performed in any case and limited just to the broken LG panel or yielded components.

Evolution of the TVT System: From the First Prototype to the 12-m-Span Glass Beam

The design of the TVTδ footbridge constitutes the final stage of a more than 10-year research period, in which three full-scale prototypes named TVTα, TVTβ, and TVTγ were designed (Fig. 3), theoretically investigated, built, and experimentally tested at the Structural Laboratory of the University of Pisa. Common key structural features are reinforcement, segmentation, prestress, hierarchy, and redundancy. However, in each development step, several expedients and improvements gradually increased the mechanical performances in order to achieve longer spans and higher safety levels

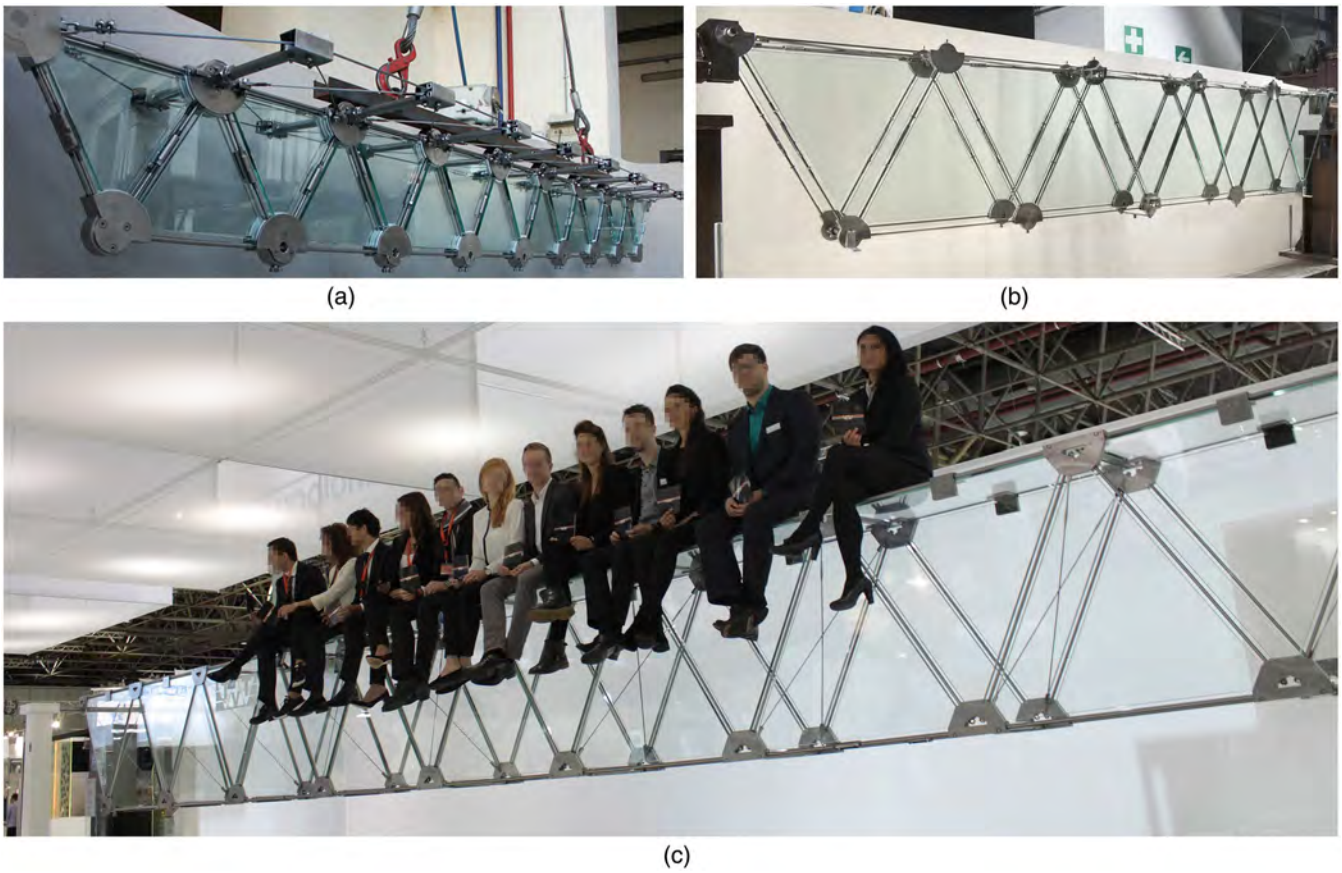

Fig. 3. TVT prototypes: (a) TVTα (2,970-mm span); (b) TVTβ (3,330-mm span); and (c) TVTγ (12,000-mm span). (Images by Maurizio Froli.)

(Fig. 4), and to facilitate assembly and replacing procedures in order to meet a cost-effective solution.

The prototype TVTα, built in 2006, was a prestressed segmented glass beam spanning 2,970 mm. The two parallel glass webs were composed by 17 equilateral triangular panels (side = 330 mm), each made of two laminated chemically tempered glass (CTG) 5-mm sheets with a 1.52-mm PVB interlayer. The height-to-span ratio was 1/9. Bars of 6 mm diameter merged in threaded holes drilled through AISI 316 steel nodes, also shaped to include the vertices of the twin glass panels. The two web layers are assembled in parallel at a short distance of 25 mm (Fig. 5). During the experimental tests, the TVTα suffered from a high deformability due to defective prestress technique. Moreover, it was also prone to lateral buckling since the beam has a T section, where the upper compressed side was equipped with a double horizontal cross cable truss.

Technical and mechanical issues found in TVTα were addressed in the TVTβ prototype, with a 3,330-mm free span, which was built and tested in 2008. A larger distance interposed between the two webs packages (190 mm) increased the lateral stability and simplified the assembly operations. The use of larger panels for a global height-to-span ratio of 1/6 allowed the whole structure to gain better SLS and ULS performances and also more transparency. Each couple of nodes was mutually connected by a tubular shaft. At the upper compressed side, the steel nodes were also diagonally connected by cables, thus forming a bracing truss (Fig. 5). Spiral stainless-steel cables replaced the prestressed bars (used in the TVTα) to facilitate assembly and prestress procedures. Tests

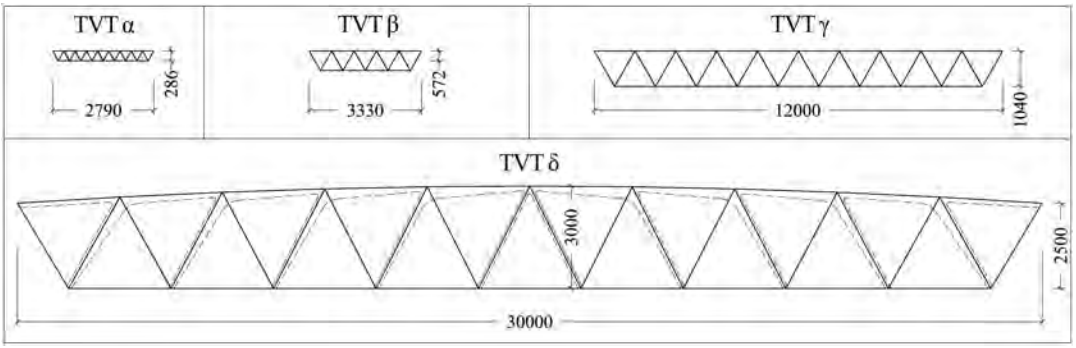

Fig. 4. Longitudinal profiles and main dimensions of the different TVT versions (unit in millimeters).

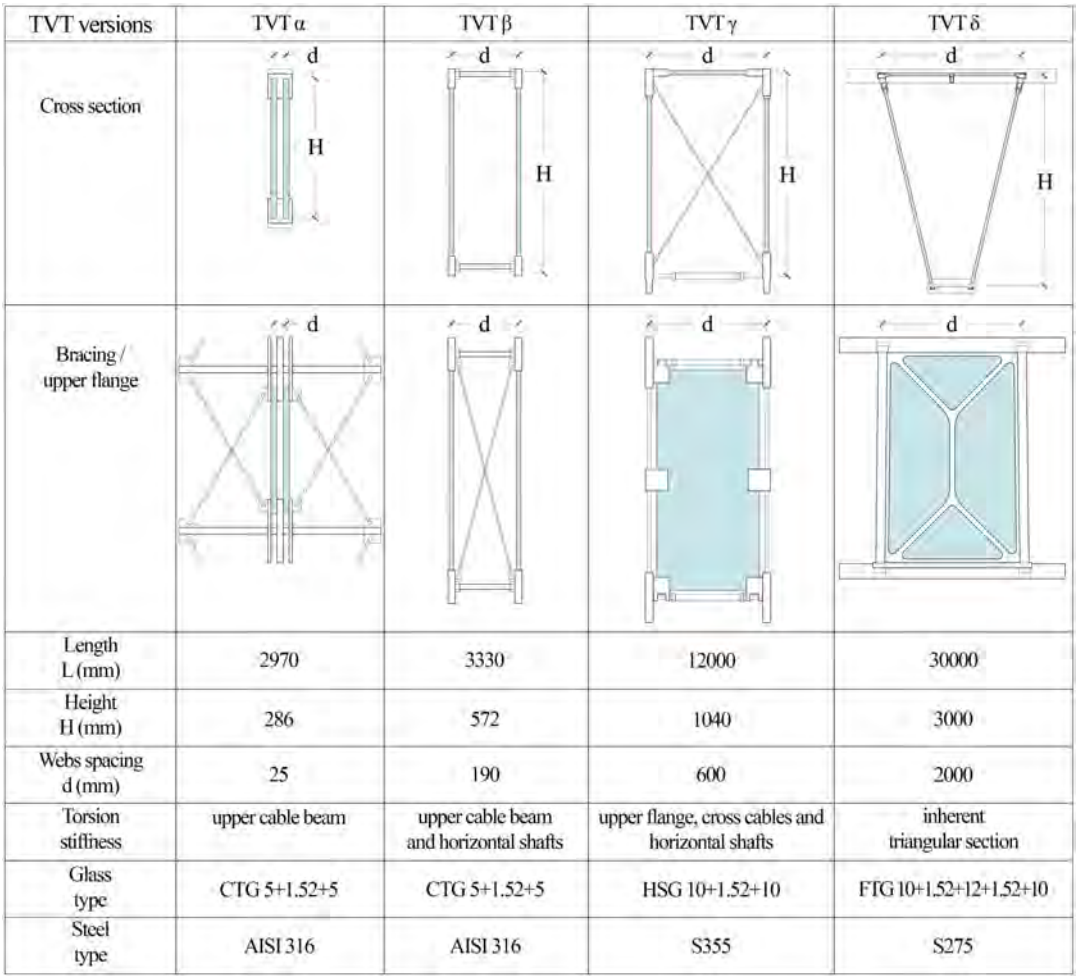

Fig. 5. Comparison of the TVT systems' technical features (unit in millimeters).

performed up to failure on TVTβ prototype (Froli and Lani 2010) confirmed the initial intuitions and theoretical calculations, thus opening the way for a third, much longer TVT exemplar.

With a span of 12,000 mm, the TVTγ prototype constituted the biggest full-scale experimentally validated glass beam in 2012. Apart from its quadrupled dimension, several substantial improvements in the nodes, connections, and mechanics differentiated the third prototype from the previous TVTα and TVTβ. The twin webs, mutually spaced at 600 mm, were both composed of a series of 19 laminated packages, each made of two 10-mm triangular heat-strengthened glass (HSG) panels with sides of 1,200 mm and 1.52-mm PVB interlayer. The two webs were connected by transversal steel shafts linking all opposite nodes. Additionally, 10 rectangular 1,200 × 600 mm LG panes, stratified as the web panels, substituted the upper cross cables of TVTβ, thus forming a segmented, compressed upper flange with the double function to increase the compressed-side area of the beam and to prevent lateral buckling (Fig. 5).

Like in the preceding prototypes, steel nodes allocated both the slots for glass panel vertices and the holes for prestressed steel bars, which replaced the TVTβ cables due to a higher stiffness demand in the assembly phase. Diagonal bars were post-tensioned by bolting their threaded extremities from a triangular cavity opened at each node center. This strategy resulted in a simpler and more effective procedure than tightening a turnbuckle as in the previous TVT beams. Because of the greater external bending moments, higher prestress forces were necessary; therefore, both bottom longitudinal bars were post-tensioned up to 30 kN by means of a hydraulic jack. A set of transversal cross cable diaphragms finally increased the torsional stiffness of the beam (Froli and Mamone 2014, Mamone 2015).

During the destructive tests of TVTγ, the yielding of lower bars occurred before the test-observed buckling failure of glass, which manifested in a single panel. Because of its increased dimensions and structural demands, a further improvement of TVTγ was the introduction of a steel clamping device at the upper flange, which connected the midlength of the glass edges and the steel bars mutually, thus considerably increasing the local buckling collapse multiplier. After the test, the yielded bars and collapsed panels were replaced, producing a new repaired specimen.

Latest Evolutionary Step: The Safety Concept of the TVTδ

The design of a TVT glass bridge (Fig. 6) points to two most relevant requirements: to assure adequate safety levels and to guarantee limited rehabilitation costs in case of glass cracking.

Concerning the first requirement, FSD and glass-steel structural collaboration are conceptually applied as in the other TVT beams, but the robustness and redundancy levels are increased. A measure introduced in the TVTδ system to provide additional redundancy and robustness is to design the steel components to behave as a skeleton. It should be stable and capable to bear at least the

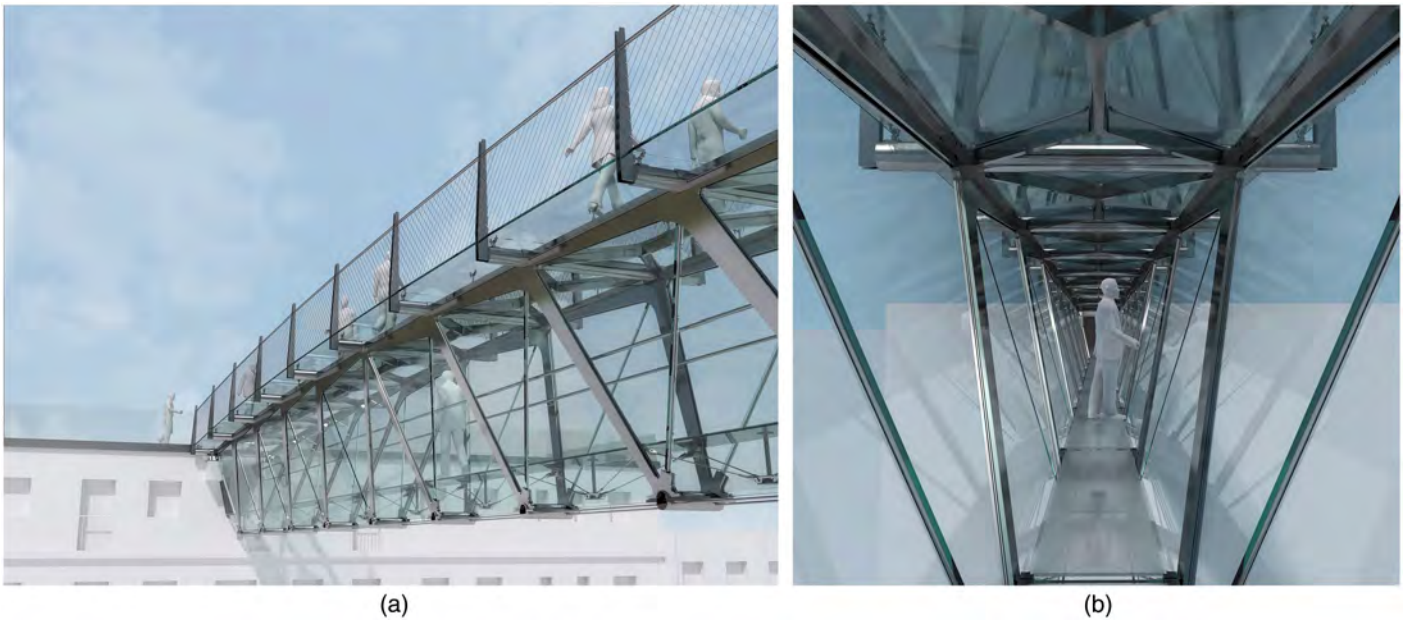

Fig. 6. 30-m span TVTδ footbridge: (a) side view; and (b) internal walk path view.

permanent load of the structure (including if possible reduced pedestrian loads) in the worst case scenario (WCS), here defined as an improbable scenario in which all glass panels break as consequence of an exceptional occurrence. To this end, compressed elements in the Warren scheme (diagonals and upper profiles) are made of steel tubes. Moreover, compared with the TVTγ, the upper flange is further segmented into a hybrid bracing made of a double Y steel tubes stiffened by triangular and trapezoidal glass panels (Fig. 6).

In the walls of the footbridge section, the tensioned elements are two pairs of lower spiral strand ropes and diagonal bars, whereas the compressed elements are hybrid trusses, which develop because of the mechanical collaboration between the steel tubes and the glass panels' edges.

A main mechanical improvement with respect to the TVTγ is the further gain in the stability of glass panels. In fact, by upscaling the cross-section size, the panels slenderness (ratio of side length over thickness) would have been in the range of 300–350 and could not be reduced by increasing the glass thickness without an excess of self-weight. On the other hand, a more efficient solution can be obtained with boomerang-shaped clamping restraint plates, which represent a development alongside the compressed edges of the midlength clamping devices adopted at the TVTγ upper flange. Additionally, because these boomerang plates are cantilevering from the tube axes, their span can be optimized proportionally to the stress magnitude at the edge of glass. So, the higher is the compression, the higher is the restraint degree to be provided in order to avoid buckling.

Buckling is prevented for both out-of-plane and in-plane unstable configurations. In the first case, the steel tube and the boomerang plates restrain the glass buckling; in the second, two adjacent glass edges restrain the in-plane buckling of the compressed steel tube (Fig. 7).

The segmented webs are inclined to create a triangular, inherently torsional-stiff cross section. Therefore, the transversal

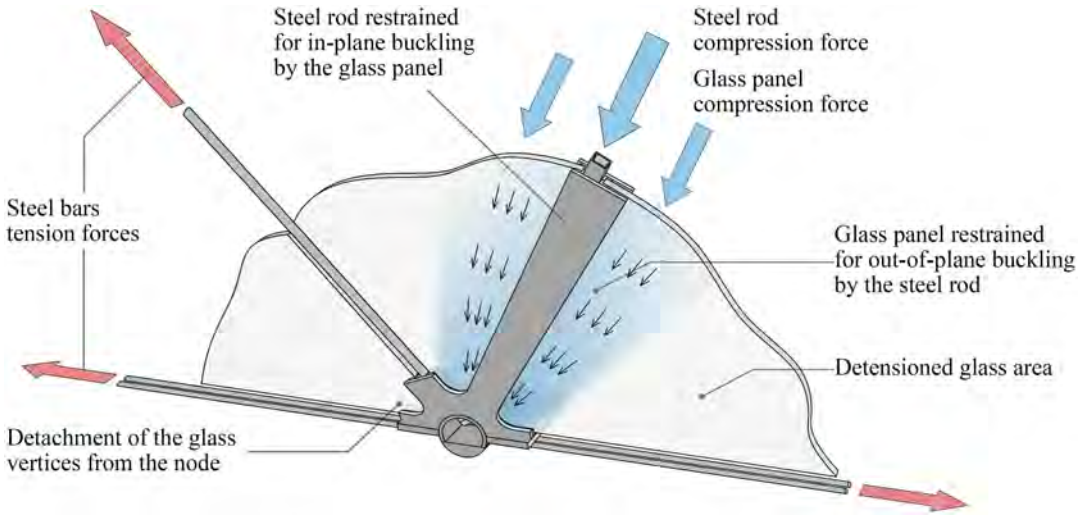

Fig. 7. Schematic equilibrium of forces representation in a lower TVTδ footbridge node.

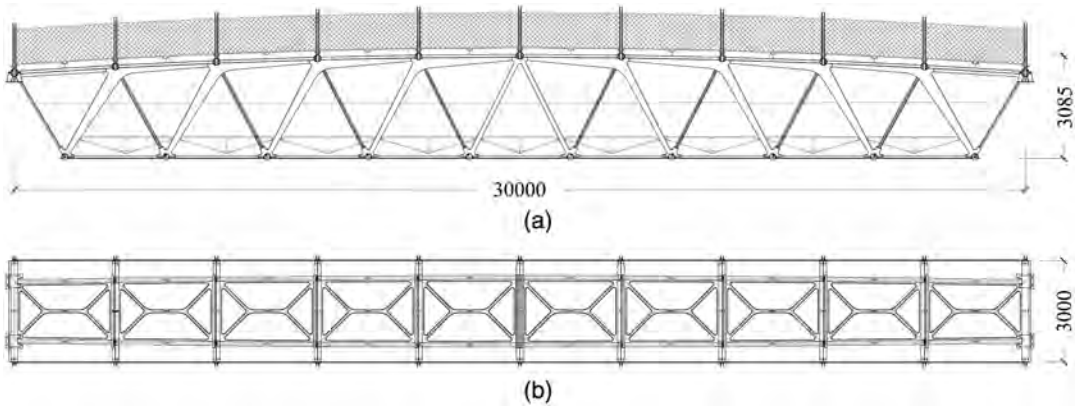

Fig. 8. TVTδ technical drawing: (a) side view; and (b) plan view (unit in millimeters).

cross-bracing cable diaphragms used in the TVTγ are no more necessary in the TVTδ. The inner space thus obtained allows the installation of a transparent walkway to be used as second path or for maintenance purposes.

In the TVTδ footbridge the upper and the inner walk paths are conceived as secondary structures, connected to the main steel skeleton, being independent from the deck and transferring just their load. Transparent glass floors are used to emphasize users' impressions, but, for safety reasons, anti-slip sacrificial transparent film is additionally provided (Fig. 6). The upper walkway is designed as a series of square LG plates, point-supported by spider steel devices. Lightweight balustrades made of cable nets are anchored to steel mullions, cantilevering from the horizontal steel shafts. The panels of the inner walk are simply laid at their corners on the steel truss and reinforced with four cables and a central strut.

Concerning the second requirement, although a fail-safe designed glass bridge dismisses the collapse of the entire construction, if the elements are single-piece or splice-laminated the occurrence of just a single crack produces economic damages comparable to global collapses. For aesthetic and psychological reasons, any other crack is not tolerable, and, even though the structure is still able to carry loads, the complete substitution of the damaged structure is normally unavoidable. On the contrary, thanks to segmentation, in TVTs it is necessary to replace only failed parts to restore the original full bearing capacity. In that case, the prestressing needs to be released and temporary works should be adopted to avoid excessive deformation.

During the structure lifetime, the nodes behave as a jointed mechanism in which the post-tensioned devices provide recentering capacity at the unloading or in case of dynamic loading. A dissipative behavior develops for cyclic external loading due to friction between the components and yielding (the latter for higher level of actions) as evidenced by the TVTβ and TVTγ experimental outcomes.

Design and Materials of a 30-m-Span TVTδ Footbridge

Geometry

The shape of the TVTδ footbridge deck is obtained from the intersection of a cylindrical surface with horizontal axis and two mirrored planes, forming an angle of 76.5° with the horizontal plane. The obtained nonuniform cross section has two orthogonal planes of symmetry. The height of the deck varies from 2,500 mm at the extremities to 3,000 mm at midspan, its planar projection from 1,760 to 2,000 mm (Fig. 8). Preserving the global static scheme of simply supported Warren beam as the other TVT exemplars, the TVTδ longitudinal upper profile results in a slightly curved arch to take benefit from an increased height at midspan. The transparency percentage, expressed as the ratio between glass area over total area, equals 81%, as observed from the side view.

The components employed in the footbridge are summarized in Table 1. The diagonal sections are optimized for material utilization and to diminish their cross-section from the supports to the midspan. The 19 web panels infill the space between the diagonals and, except for the isosceles central panel, all triangles are scalene with side dimensions in the range of 2,973–2,446 mm (from midspan to extremities) and angles from 64° to 52°. All panels have rounded vertices, which are included in monolateral nodes with aluminum alloy as interposed softer material (see the section "Materials" for details), to avoid stress peaks, following the same concept of preceding TVT beams. The spacers are also continuously provided within the boomerang clamping.

Table 1. Main components of the TVTδ footbridge deck

Component	Material	Type/section	Dimension
Upper profile	S275 steel	Hollow square with boomerangs	Variable
Compressed diagonal	S275 steel	Hollow square with boomerangs	Variable
Tensioned diagonal	S275 steel	Bars with threaded extremities	Variable
Lower profile	Steel	Spiral strand rope	$4 \times \Phi 26$ mm
Web glass panels	Laminated FTG	Laminated triangular panel with rounded corners	$10 + 12 + 10$ mm with 1.52 PVB interlayer
Double Y profile	S275 steel	Hollow rectangular with continuous clamping	RHS $100 \times 50 \times 8$ mm
Transversal shaft	S275 steel	Hollow tube	CHS 202.8×7.5 mm
Upper flange glass panels	Laminated FTG	Laminated triangular and trapezoidal panels with rounded corners	$12 + 12$ mm with 1.52 PVB interlayer

Note: CHS = circular steel hollow section; FTG = fully tempered glass; and RHS = rectangular steel hollow section.

Construction Method

The footbridge is partially fabricated in the shop and dry assembled on site, then post-tensioned and installed onto the supports. A schematic view of the assembly procedure is shown in Fig. 9. The basic preassembled skeleton modules are made of two compressed diagonals, two bars (tensioned diagonals) reciprocally linked at the lower node, and two upper longitudinal profiles interposed between a transversal tubular shaft and a female coupling plate. The lower strand ropes can be inserted. The steel modules can be reciprocally merged by fastening the shaft on the female coupling plate. Once all the modules are assembled, the upper plates (double Y steel profile and panels) and the web panels can be installed by means of a simple translational movement. Then, they can be locked in place by means of specific carters and removable external boomerang plates, respectively. The diagonal bars can be adjusted and post-tensioned by bolting the threaded extremities from the cavities located in both the upper shaft and the lower node, guaranteeing contact of all components.

The rounded vertices and edges of the glass panes, which are in-plane and out-of-plane in contact with steel, are equipped with C-shaped aluminum alloy spacers that wrap the compressed panel edges. Because both upper and lower nodes constitute a relevant load transfer device, solid sections and thick plates are adopted to transfer compression loading to the glass panels (Fig. 10).

The strand ropes are initially sliding. After their post-tensioning by means of a removable contrast rig, they can be locked in place by fastening the wedges at all intermediate lower nodes. The anchor points of the TVTδ footbridge are pins made of stiffened steel hinges able to clamp the extreme shafts of the structure. After the construction of the deck, the glass panes of the internal and external walkway can be fastened.

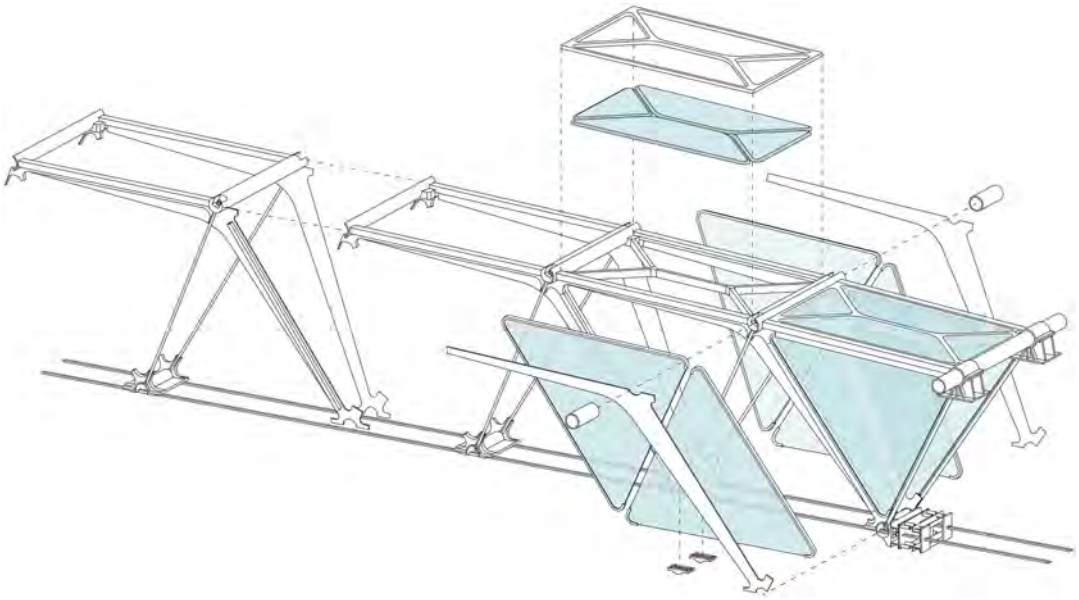

Fig. 9. Schematic assembly and post-tensioning of the footbridge.

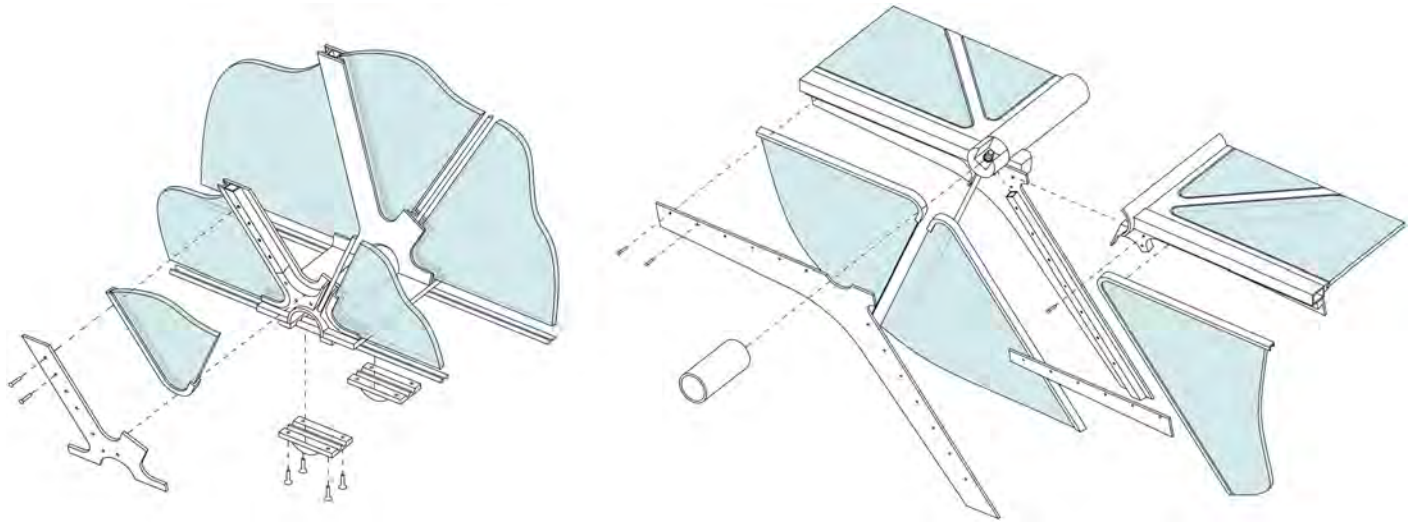

Fig. 10. Schematic assembly of upper and lower nodes.

Like in the previous TVT exemplars, the dry, reversible assembly allows easy and money-saving replacement of eventually damaged glass panels after releasing the post-tensioned strand ropes. Furthermore, the skeleton of the structure, beyond its safety function, avoids using any scaffolding in the erection phase. So each panel can be individually assembled and removed.

Materials

To maximize the economy of the system, standardized or commercial products and materials are employed. Table 2 summarizes the materials constituting the footbridge. Properties have been drawn from codes and standards (Feldmann et al. 2014).

Modeling and Analysis

The 30-m TVTδ footbridge is numerically described by means of FE models with the aim to assess the strength, stiffness, and stability of the structure at both the global and the local level.

Table 2. Mechanical characteristics of the materials included in the FEM models

Material	Property	Value
Steel S275[a]	Young's modulus, E	210 GPa
	Yielding strength, f_{yk}	275 MPa
Steel strand ropes[b]	Young's modulus, E	150–170 MPa
	Ultimate tensile force, F_{tk}	621 kN
	Yielding force, F_{yk}	376 kN
Aluminium alloy[c]	Young's modulus, E	70 GPa
Glass FTG	Young's modulus, E	70 GPa
	Tensile strength, f_{gk}	120 MPa
	Compressive strength	800 MPa

[a]Steel type to comply with EN 10025 (CEN 2005c).
[b]Commercial product.
[c]Aluminium type to comply with EN AW 6060 T5 (CEN 2005a).

A multiscalar strategy from local to global was adopted. The steel components are initially sized for the skeleton behavior by means of analytical calculations derived from the Warren scheme model, whereas the glass components are designed at buckling by means of FE local models.

Then, a three-dimensional model of a quarter of the footbridge is developed within the Straus7 package because of the double half-symmetry for both geometry and loads.

Thin shell elements are used to model glass panels and steel nodes; the remaining steel components, tubes, and bars are modeled as beam elements, whereas the cables are modeled as a truss. The upper and compressed diagonal sections have equivalent properties in order to include the contribution of the boomerangs. Concerning boundaries, extreme joints are pinned, and appropriate conditions assured the symmetry along the transversal and the longitudinal midplanes.

The dead load is automatically affixed by setting up the material properties. The live loads, concentrated forces at the upper steel nodes, are increased at each load step according to Eurocode load combinations (CEN 2005b). The adopted mesh is four-node quadrilateral (Quad4). Nodes, compressed diagonals, and longitudinal upper elements are linked to the edge nodes of the glass panel by in-plane monolateral point contact elements to simulate the compression-only contact between steel and glass as well as the presence of the spacers. Out-of-plane displacements of both elements are constrained due to the presence of the boomerangs. Glass panels are modeled as equivalent glass thickness plates with linear elastic material property. The model is fully descriptive of the stress state of the structure and of the contact between all the components. The model building, especially regarding the glass panes and element contacts, was assisted by the TVT state-of-the-art data set, namely experimental outcomes and modeling experience (i.e., Froli et al. 2017).

Nonlinear analyses are performed considering material, contact, and geometric nonlinearities. Two FE models are presented and discussed with the following purposes (Fig. 11).

- Hybrid model: It includes all components, and glass is both reinforced and post-tensioned. The purpose is to assess the ULS

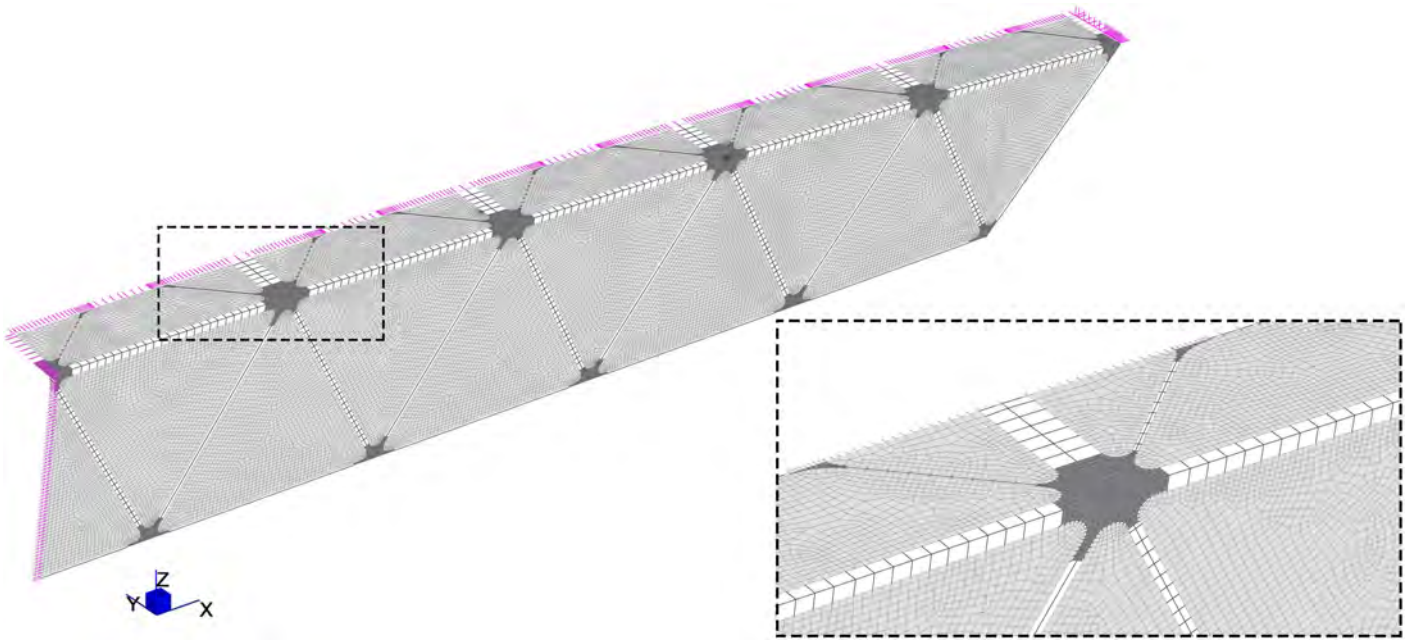

Fig. 11. FEM model of the TVTδ footbridge.

strength and ductility and the stress field on the glass panels within all load phases; and

- WCS model: It consists in the same hybrid model in which the glass panels had null stiffness, and consequently they are considered only as a dead load. The purpose is to assess the WCS. Same FEs and links as in the detailed model are adopted.

An effective comparison for these two models concerned the ULS performances of the steel components, to highlight the mechanical contribution of glass, and the SLS midspan deflection of the footbridge to compare the residual stiffness of both systems.

The buckling of panels is estimated through extracted portion of the structure, reproducing the most stressed panes in compression with boundary conditions given by the hybrid model.

The natural frequency analysis is performed on a full finite-element method (FEM) model of the footbridge, in which the contacts are linearized because small displacement theory applies. However, initial conditions for the analysis are provided by Phase 0 load combination, i.e., including the effect of post-tensioning.

Result and Discussion

The analyses results obtained from the hybrid model are presented and commented with reference to Phases 0, 1, and 2 (Figs. 12 and 13). The results from both setups (hybrid and WCS) are then compared at the ULS and SLS. Local models for buckling and dynamic model for natural frequency analysis are included in separated paragraphs.

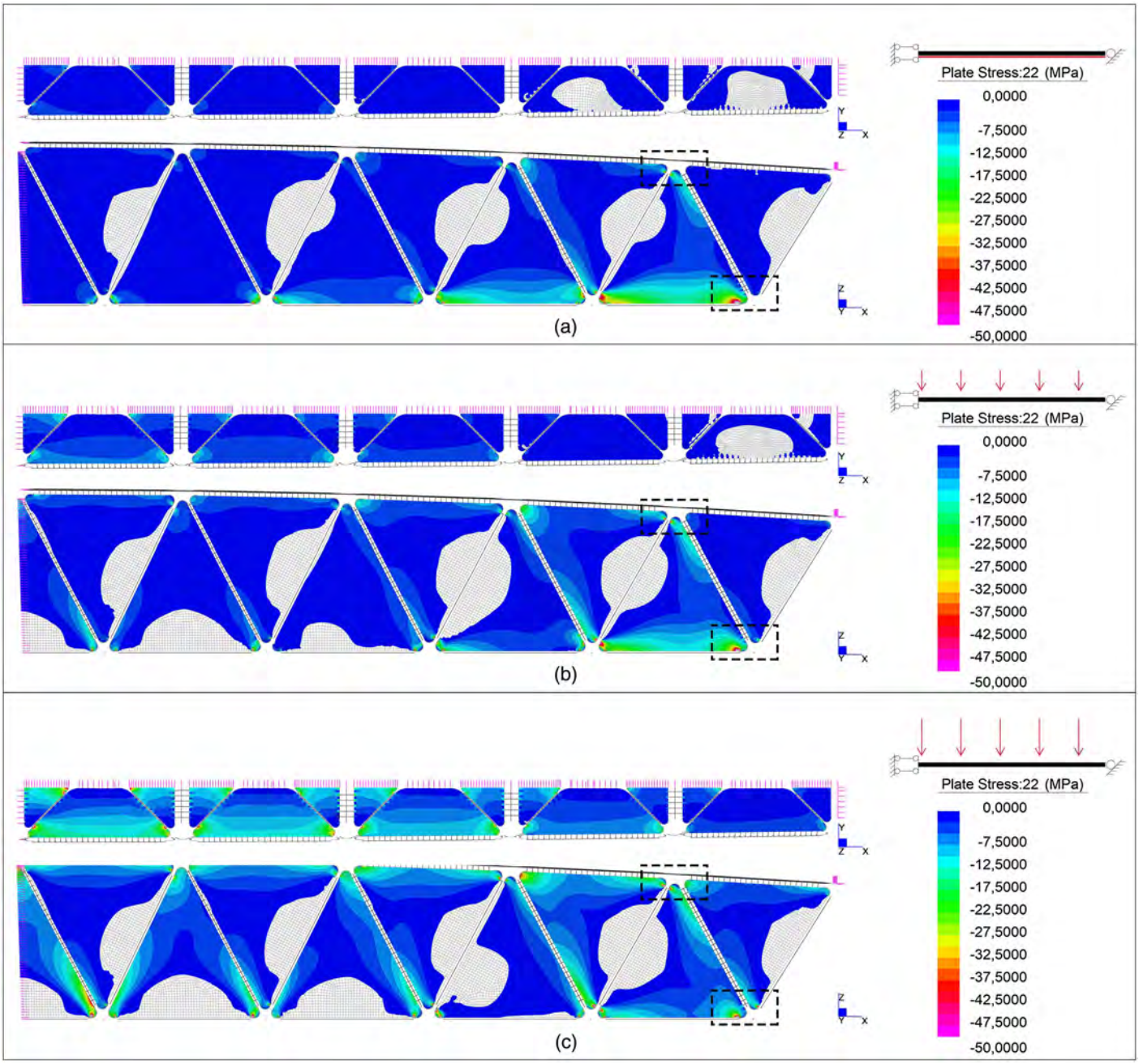

Fig. 12. Detailed model results: minimum principal stress on the glass panels within (a) Phase 0 (assembly); (b) Phase 1 (SLS); and (c) Phase 2 (ULS). Peak values are excluded from the contour map and shown for the highlighted areas only in Fig. 13.

J. Bridge Eng., 2020, 25(1): 04019117

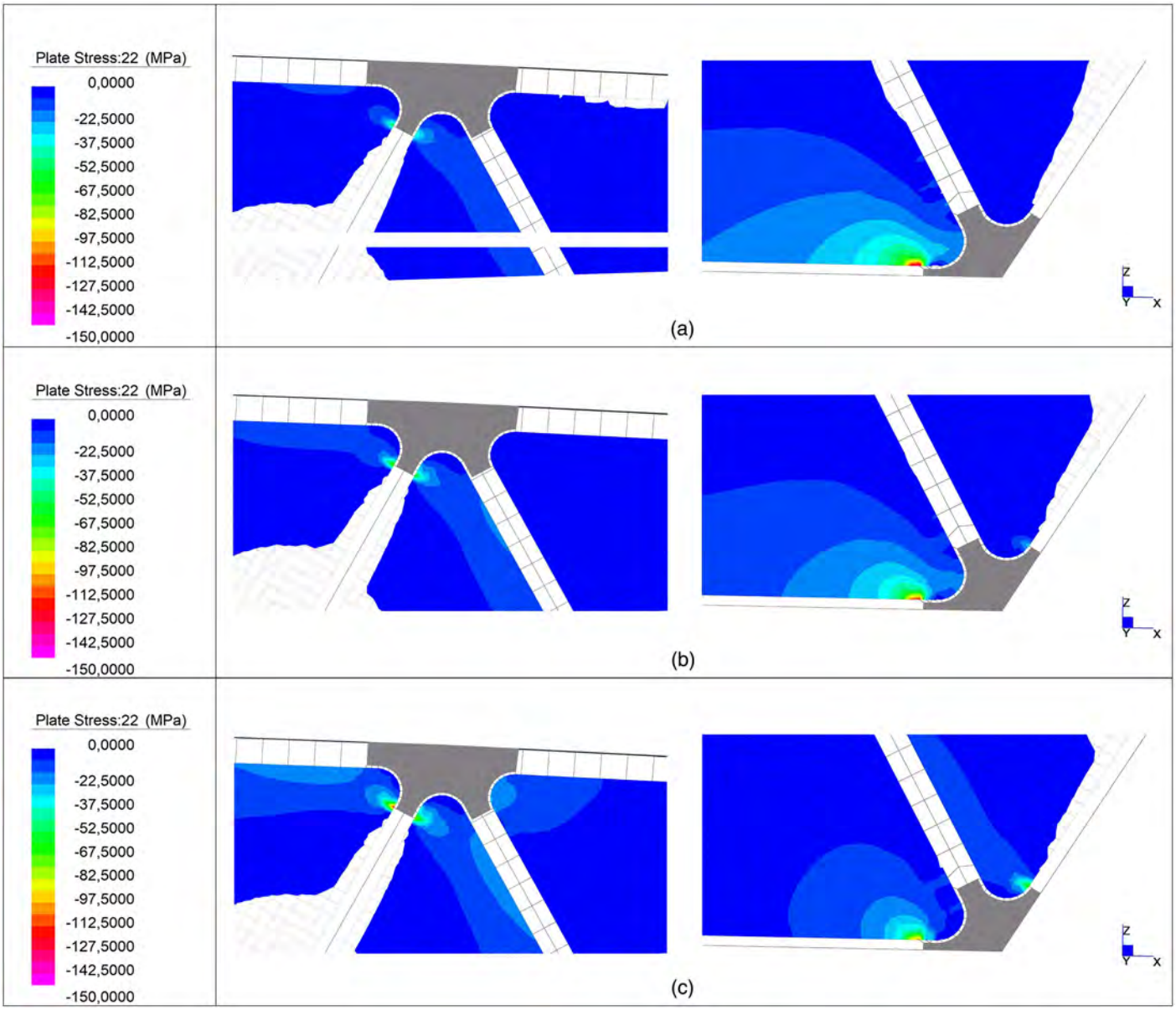

Fig. 13. Detailed model results: minimum principal stress in the nodes surrounding within (a) Phase 0 (assembly); (b) Phase 1 (SLS); and (c) Phase 2 (ULS) (with reference to Fig. 12).

Stress Field on Panels

Phase 0 represents the assembly of the structure, in which the structure is submitted to dead and nonstructural loads, and post-tensioning of cables is practiced. The midspan deflection due to the dead and nonstructural loads is almost entirely balanced by the post-tensioning action. Glass is mostly compressed as evidenced in Figs. 12 and 13, in which the minimum principal stress is plot. Higher absolute values up to a peak of 115 MPa develop at the lower node of the extremity panel, in which the maximum is both the shear and the post-tensioning loading due to the adjacency to the load-introduction node. Such peak value diminishes in the subsequent phases. Both upper and lower glass corners are in contact with the steel nodes because spacer elements have compressive axial stress (Fig. 13).

Phase 1 represents the structure under SLS load combination. Decompression of glass is caused by these loads, and spreads from midspan to the extremities. Lower edges of panels (Fig. 12) better catch this effect. Hence, at the midspan panel, these areas are almost entirely unloaded. Overall, the maximum principal tensile stress is below the safety threshold, while the compression stresses increase along the edges of the extreme panels.

Phase 2 identifies the ULS of the structure, in which the lower strand is approaching its yielding state. Moreover, the progressive decompression of glass panel at the corners induces their detachment from the node cavities. So, because of the compression-only nature of gaps, several elements resulted as inactive. Accompanying tensile stresses due to large displacement develop in these zones. The compression stresses thicken around the Warren compressed struts while the remaining areas are unloaded, in compliance with the scheme shown in Fig. 7. Tensile forces are mostly sustained by the steel components.

WCS Behavior

The WCS behavior is evaluated by analyzing the WCS model. Hence, the safety factors in the two extreme failure scenarios

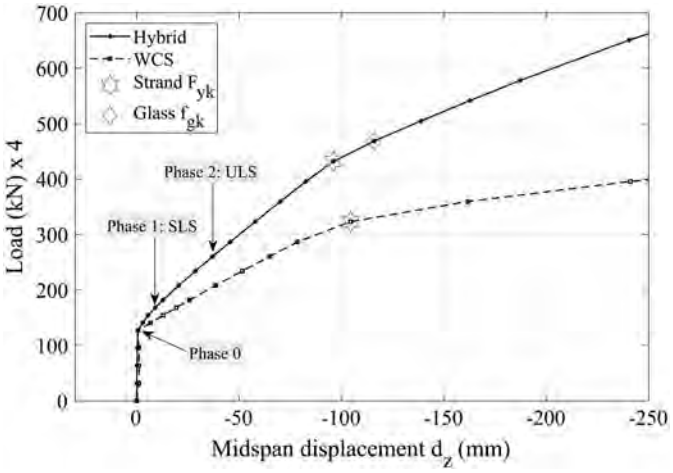

Fig. 14. Load–displacement curve comparison for the hybrid and WCS models.

are compared: (1) the ULS of the footbridge, in which the lower strands are approaching the yielding state but all glass panels still contribute in the load bearing; and (2) the WCS, in which all glass panels are supposed to be collapsed and regarded as a dead load, and only steel components carry loads. Moreover, as a measure of the residual stiffness of both systems, the midspan deflection at the SLS load combination is evaluated. In conclusion, by comparing these scenarios, it is possible to isolate quantitative information about the redundancy offered by the structure at the ULS and the advantage of hybrid collaboration at the SLS.

The results are shown in Fig. 14 and are summarized in Table 3. Two curves in Fig. 14 plot the total vertical load on a quarter of the footbridge versus the midspan displacement, one curve for the hybrid case and one for the WCS case. Concerning stiffness, the contribution of glass appears evident because the curves significantly deviate from Phase 0 forward. Even from this point, the decompression of glass at SLS is also visible due the reduction of stiffness.

Concerning strength, the yielding of the strand occurs at about 1.5 times the ULS load in the hybrid case, but at about 1.2 times the ULS load in the WCS case. The characteristic value of glass tensile strength is exceeded at about 1.6 times the ULS load (hybrid case only), stating a hierarchy in the chain of failure in the hybrid system according to DAD philosophy, at least in terms of characteristic values. From that point forward the curve is expected to be flatter than it is due to progressive reduction of stiffness of cracked panes. However, the phenomenon of glass failure is not included in such a global model and glass has a linear infinitely elastic behavior. Glass design strength values are in any case above the ULS point in the plot.

Concerning the ductility of the system, the yielding of the lower strand matches with a visible change of stiffness and leads to a global ductile behavior for both the hybrid and WCS cases.

Expressing the safety factor as the ratio of the maximum tension and compression over the element strength (Table 3), values of 1.37 and 11.11 are respectively obtained at ULS, and 1.06 and 4.55 in the WCS. From their ratio, the redundancy of the system with respect to the WCS can be measured as +29%.

At SLS, the normalized midspan deflection is about doubled in the WCS with respect to hybrid SLS condition. Therefore, the stiffness contribution given by the panels can be identified as +49%.

Table 3. Main results from the hybrid and WCS models

Model	ULS tension safety factor, λT	ULS compression safety factor, λC	SLS normalized displacement, $\kappa\delta$
ULS	1.37	11.11	0.51
WCS	1.06	4.55	1.00
ULS/WCS	1.29	2.44	0.51

Glass Panels Buckling

Because the glass panels are compressed, a possible failure scenario is buckling. The most critical panels identified among the most slender and the most loaded are extracted from the assembly and then analyzed with their equivalent thickness through linear buckling analysis. No geometrical imperfection is considered on the panels because the response of triangular laminated glass panels in-plane and out-of-plane loaded is an unexplored research area (Laccone et al. forthcoming); however, the displacement field caused by their dead load acts as an initial imperfection. Restraints for the panes are in-plane edge supports and out-of-plane elastic supports, simulating boomerang plates and nodes clamping. A force is applied on a vertex of the panel, whose magnitude is equivalent to the vector sum of the ULS axial load of the point contact.

Referring to Fig. 15, all panes are clamped at their vertices. Moreover, Panel A is out-of-plane restrained by the boomerang plates along the upper edge and the diagonal edge. Its buckling multiplier results as 28.69. Panel B is smaller than Panel A and is restrained just along one diagonal edge. However, it resulted as more compressed due to shear, and so it has a buckling factor of 7.74. In both cases, buckling occurs for a higher level of external load with respect to the ULS of the footbridge.

Dynamic Behavior

The study of the dynamic behavior of the TVTδ footbridge is based on the natural frequency analysis performed by means of an FEM model representing the whole structure. The output data is discussed in the perspective of the supposed pedestrian traffic and vibration comfort demands because, being a lightweight structure, the present bridge type can be susceptible to vibration when submitted to dynamic pedestrian footfall.

Fig. 16 represent modal shapes of relevant modes. Natural frequencies and participating mass of the first 20 modes are collected in Table 4.

A preliminary check on main frequencies before evaluating the accelerations on the footbridge can be performed according to Heinemeyer and Feldmann (2009). The first vibrations for both vertical and horizontal modes $f_2 = 3.452$ Hz and $f_1 = 2.866$ Hz are outside the ranges of *lively bridges*, which are $1.3 \le f_i \le 2.3$ Hz and $0.5 \le f_i \le 1.2$ Hz, respectively. Moreover, according to SETRA (2006), the risk of resonance is low for standard loading situations in the case of vertical vibration and negligible in the case of lateral vibration.

Bearing in mind that the perception of vibrations is subjective and strongly depends on variables related to the structure and to the user, a further step is to evaluate comfort thresholds in relation to peak accelerations occurring for certain load scenarios. The TVTδ footbridge is supposed to be a Class III or II footbridge, a normally used footbridge that can sometimes be crossed by large groups, but never loaded over its whole area, or urban footbridge, subjected to heavy traffic and that may occasionally be loaded throughout its bearing area, respectively (SETRA 2006). In both scenarios of sparse and dense crowd (density d equal to 0.5 or 0.8 pedestrians/m^2, respectively), there is no risk of resonance

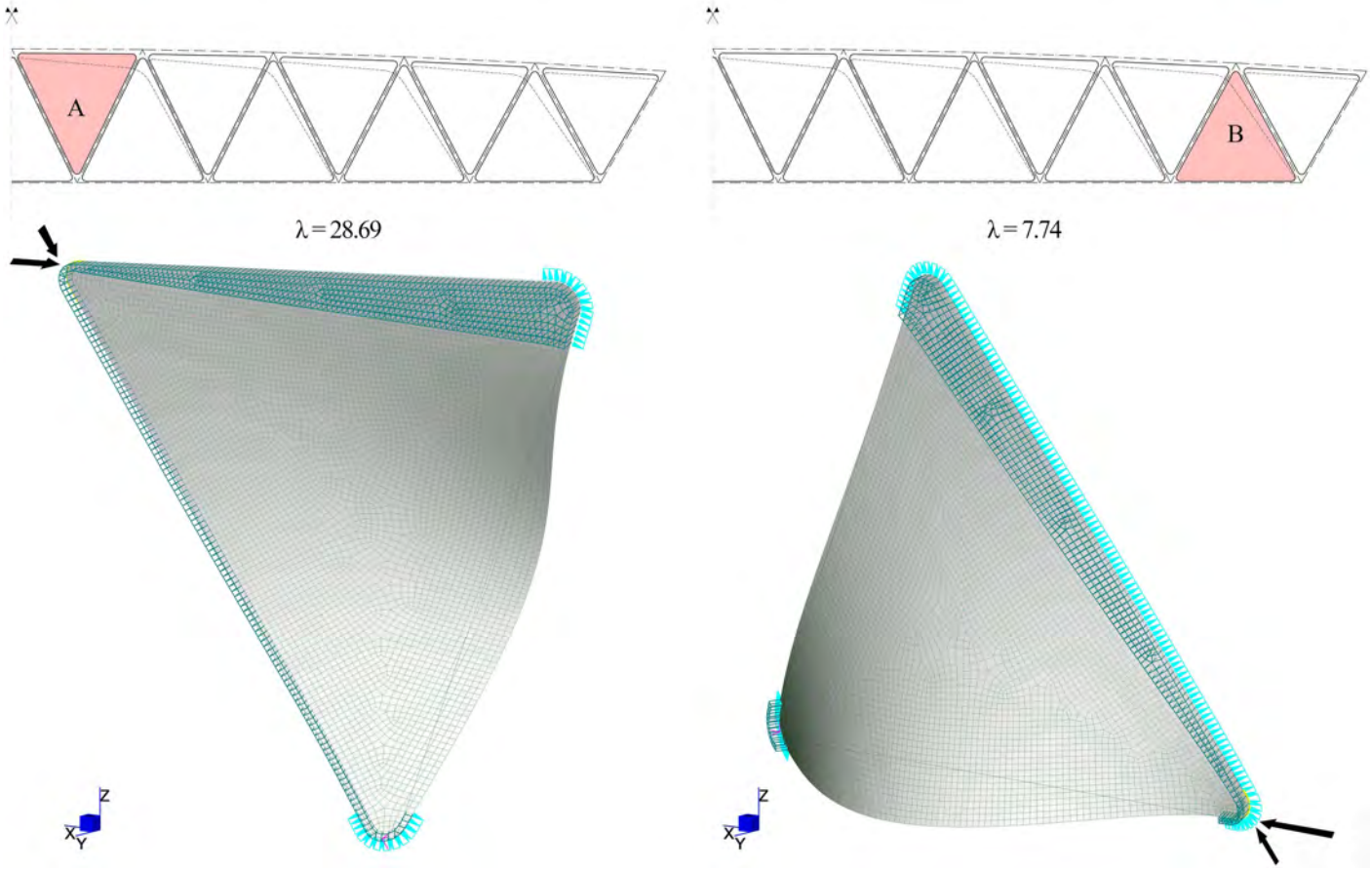

Fig. 15. Local buckling analysis of the most compressed TVTδ glass panels.

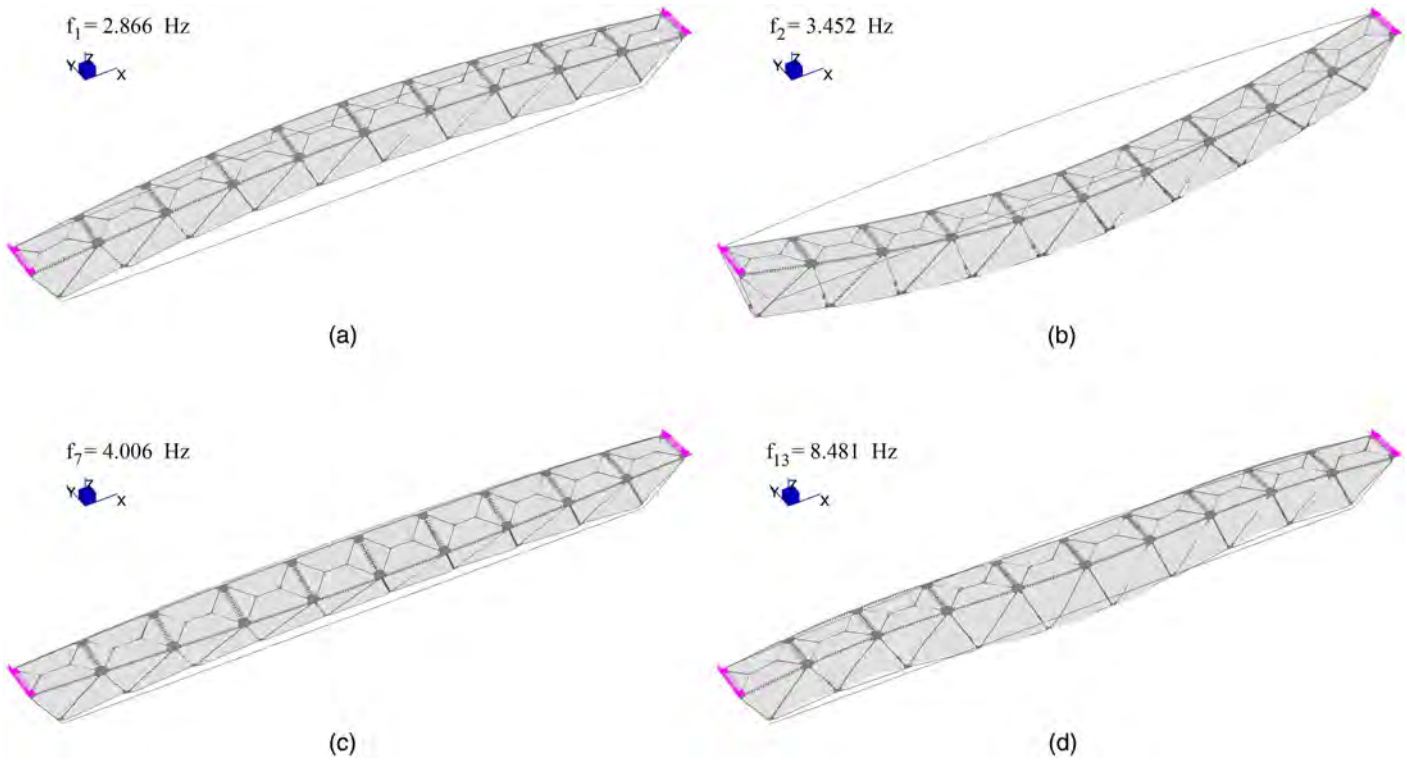

Fig. 16. Main modal shapes: (a) Mode 1 (lateral); (b) Mode 2 (vertical); (c) Mode 7 (torsional); and (d) Mode 13 (lateral).

Table 4. Natural frequencies and mass participation factors deduced from the FEM full model

Mode	Frequency (Hz)	Mx (%)	My (%)	Mz (%)
1	2.866	0.00	80.64	0,00
2	3.452	0.00	0.00	83,57
3	3.933	0.00	0.09	0,00
4	3.937	0.00	0.00	0,00
5	3.939	0.00	0.00	0,00
6	3.939	0.00	0.00	0,00
7	4.006	0.00	2.52	0,00
8	6.000	0.00	0.00	0,00
9	7.456	0.00	0.00	0,00
10	7.456	0.00	0.00	0,00
11	7.456	0.00	0.00	0,00
12	7.456	0.00	0.00	0,00
13	8.481	0.00	7.25	0,00
14	9.310	0.00	0.00	0,00
15	10.250	0.00	0.00	0,00
16	11.010	0.00	0.07	0,00
17	11.020	0.00	0.00	0,00
18	11.020	0.00	0.00	0,00
19	11.020	0.00	0.00	0,00
20	11.110	0.00	1.81	0,00
Total mass participation factors		0.00	92.37	83.57

Note: Mx, My, Mz are mass participation factors with reference to axes in Fig. 16.

neither in the main direction of vibration nor due to the second-harmonic-of-the-crowd effect.

Conclusion

The TVTδ hybrid glass-steel footbridge is the engineering response to the demand for evanescent structures and a weightless walk path. Apart from its mechanical characteristics, this concept is also the expression of a holistic vision of the structure as architecture and landmark. The 10-year TVT research program has provided progressive confidence in the system capabilities and several technical and mechanical improvements, which consequently produced progressively longer free spanned highly transparent structures. The TVTδ footbridge matches the specific material mechanics of both glass and steel, and their mechanical collaboration results in a lightweight and optimized solution. The feasibility is assessed by numerical analyses calibrated on the data set of previous TVT prototypes, from which it can be concluded that the TVTδ footbridge has an appropriate safety margin and manifests a ductile failure, even using such a fragile material like glass.

Data Availability Statement

Some or all data, models, or code generated or used during the study are proprietary or confidential in nature and may only be provided with restrictions. TVT is a patented product. FEM models can be provided for research purposes.

Acknowledgments

The authors of this paper were awarded with a Merit Award and ranked 2nd place in the International Competition WIBE Prize (World Innovation in Bridge Engineering) 2017 edition, with a project entitled "The TVT δ 'Rainbow' bridge: A new technique for long-spanned, highly transparent footbridges." The four juries were constituted by members indicated by the International Association for Bridge and Structural Engineering (IABSE), Fédération internationale du béton (fib), International Association for Bridge Maintenance and Safety (IABMAS), AISC, European Council of Civil Engineers (ECCE), and ASCE. This paper has been published with the permission of the WIBE Committee. The first author wishes to acknowledge the following people for their contribution in the development of the TVT prototypes: D. Pardini, S. Serracchiani, A. Russo, L. Lani, G. Masiello, V. Mamone, M. Giammattei, and D. Maesano.

References

Aurik, M., A. Snijder, C. Noteboom, R. Nijsse, and C. Louter. 2018. "Experimental analysis on the glass-interlayer system in glass masonry arches." *Glass Struct. Eng.* 3 (2): 335–353. https://doi.org/10.1007/s40940-018-0068-7.

Bos, F. P. 2009. "Safety concepts in structural glass engineering: Towards an integrated approach." Ph.D. thesis, Dept. of Building Technology, TU Delft.

Bos, F. P., F. A. Veer, G. J. Hobbelman, and P. C. Louter. 2004. "Stainless steel reinforced and posttensioned glass beams." In *Proc., 12th Int. Conf. of Experimental Mechanics (ICEM12)*. Milan, Italy: McGraw-Hill.

CEN (European Committee for Standardization). 2005a. *Aluminium and aluminium alloys – Extruded precision profiles in alloys EN AW-6060 and EN AW-6063*. EN 12020-2:2016. Brussels, Belgium: CEN.

CEN (European Committee for Standardization). 2005b. *Eurocode: Basis of structural design.* EN 1990:2002. Brussels, Belgium: CEN.

CEN (European Committee for Standardization). 2005c. *Hot rolled products of structural steels – Part 1: General technical delivery conditions*. EN 10025-1. Brussels, Belgium: CEN.

Cupać, J., K. Martens, A. Nussbaumer, J. Belis, and C. Louter. 2017. "Experimental investigation of multi-span post-tensioned glass beams" *Glass Struct. Eng.* 2 (1): 3–15. https://doi.org/10.1007/s40940-017-0038-5.

Dotan, H. 2016. "Zhangjiajie Grand Canyon glass bridge." In Vol. 5 of *Proc., Challenging Glass Conf.*, 3–12. Ghent, Belgium: Ghent Univ.

Engelmann, M., and B. Weller. 2016. "Post-tensioned glass beams for a 9 m Spannglass bridge." *Struct. Eng. Int.* 26 (2): 103–113. https://doi.org/10.2749/101686616X14555428759000.

Feldmann, M., et al. 2014. *Guidance for European structural design of glass components*. Brussels, Belgium: Publications Office of the European Union.

Feng, R. Q., Y. Jihong, and Y. Yao. 2015. "A new type of structure: Glass cable truss." *J. Bridge Eng.* 20 (12): 04015024. https://doi.org/10.1061/(ASCE)BE.1943-5592.0000734.

Froli, M., and F. Laccone. 2018a. "Static concept for long-span and high-rise glass structures." *J. Archit. Eng.* 24 (1): 04017030. https://doi.org/10.1061/(ASCE)AE.1943-5568.0000285.

Froli, M., and F. Laccone. 2018b. "Hybrid GLAss-steel stele (HYGLASS): Preliminary mechanical study on a smart tetrahelical cantilevering tall structure." In Vol. 6 of *Proc., Challenging Glass Conf.*, 611–616. Delft, Netherlands: TU Delft Open.

Froli, M., F. Laccone, and D. Maesano. 2017. "The TVT glass pavilion: Theoretical study on a highly transparent building made with long-spanned TVT portals braced with hybrid glass-steel panels." *Buildings* 7 (4): 50. https://doi.org/10.3390/buildings7020050.

Froli, M., and L. Lani. 2010. "Glass tensegrity trusses." *Struct. Eng. Int.* 20 (4): 436–441. https://doi.org/10.2749/101686610793557564.

Froli, M., and V. Mamone. 2014. "A 12 meter long segmented, post-tensioned steel-glass beam (TVT Gamma). In *Proc., Challenging Glass 4 & COST Action TU0905 Final Conf.*, 243–251, edited by C. Louter, F. Bos, and J. Belis. London: Taylor & Francis Group.

Haldimann, M., A. Luible, and M. Overend. 2008. *Structural use of glass*. Zürich, Switzerland: International Association for Bridge and Structural Engineering.

Heinemeyer, C., and M. Feldmann. 2009. "European design guide for footbridge vibration." In *Footbridge vibration design*, 13–30. Boca Raton, FL: CRC Press.

Laccone, F. 2019. "Reinforced and post-tensioned structural glass shells. Concept, morphogenesis and analysis." Ph.D. thesis, Dept. of Energy, Systems, Territory, and Construction Engineering, Univ. of Pisa.

Laccone, F., C. Louter, and M. Froli. Forthcoming. "Glass-steel triangulated structures: Parametric nonlinear FE analysis of in-plane and out-of-plane structural response of triangular laminated glass panels." *J. Archit. Eng.* https://doi.org/10.1061/(ASCE)AE.1943-5568.0000374.

Louter, C., J. Belis, F. Veer, and J.-P. Lebet. 2012. "Structural response of SG-laminated reinforced glass beams; experimental investigations on the effects of glass type, reinforcement percentage and beam size." *Eng. Struct.* 36 (Mar): 292–301. https://doi.org/10.1016/j.engstruct.2011.12.016.

Mamone, V. 2015. "Experimental, numerical and analytical investigations on the segmented post-tensioned hybrid steel-glass beams TVT." Ph.D. thesis, Dept. of Civil Engineering, Univ. of Pisa.

Martens, K., R. Caspeele, and J. Belis. 2015a. "Development of composite glass beams—A review." *Eng. Struct.* 101: 1–15. https://doi.org/10.1016/j.engstruct.2015.07.006.

Martens, K., R. Caspeele, and J. Belis. 2015b. "Development of reinforced and posttensioned glass beams: Review of experimental research." *J. Struct. Eng.* 142 (5): 04015173. https://doi.org/10.1061/(ASCE)ST.1943-541X.0001453.

Nijsse, R. 2003. *Glass in structures: Elements, concepts, designs*. Boston: Birkhäuser.

Oikonomopoulou, F., T. Bristogianni, F. A. Veer, and R. Nijsse. 2018. "The construction of the Crystal Houses façade: Challenges and innovations." *Glass Struct. Eng.* 3 (1): 87–108. https://doi.org/10.1007/s40940-017-0039-4.

Royer-Carfagni, G., and M. Silvestri. 2007. "A proposal for an arch footbridge in Venice made of structural glass masonry." *Eng. Struct.* 29 (11): 3015–3025. https://doi.org/10.1016/j.engstruct.2007.01.031.

SETRA (Service d'Études Techniques des Routes et Autoroutes). 2006. *Footbridges: Assessment of vibrational behaviour of footbridges under pedestrian loading*. Paris: SETRA.

Vallee, T., C. Grunwald, L. Milchert, and S. Fecht. 2016. "Design and dimensioning of a complex timber-glass hybrid structure: The IFAM pedestrian bridge." *Glass Struct. Eng.* 1 (1): 3–18. https://doi.org/10.1007/s40940-016-0007-4.

Veer, F. A., et al. 2003. "Spanning structures in glass." In *Glass processing days*, 78–81. Tampere, Finland: Glaston OYJ.

Wittenberg, D., and M. Krynski. 2010. "Design of a single span nine metre long glass bridge." In Vol. 2 of *Proc., Challenging Glass Conf.*, 225–231. Delft, Netherlands: TU Delft Open.